ISSN 1063-7826, Semiconductors, 2023, Vol. 57, No. 6, pp. 300–304. © Pleiades Publishing, Ltd., 2023.
Russian Text © The Author(s), 2022, published in Fizika i Tekhnika Poluprovodnikov, 2022, Vol. 56, No. 11, pp. 1082–1087.
English Text © Ioffe Institute, 2022.

Influence of Source Composition on the Planar Growth of Nanowires during Catalytic Growth in a Quasi-Closed Volume

L. B. Karlina[a],*, A. S. Vlasov[a], I. P. Smirnova[a], B. Ya. Ber[a], D. Yu. Kazantsev[a], M. V. Tokarev[a], and I. P. Soshnikov[a,b,c]

[a] *Ioffe Institute, St. Petersburg, 194021 Russia*
[b] *Alferov Federal State Budgetary Institution of Higher Education and Science Saint Petersburg National Research Academic University of the Russian Academy of Sciences, St. Petersburg, 194021 Russia*
[c] *Institute of Analytical Instrument Making, Russian Academy of Sciences, St. Petersburg, 190103 Russia*
**e-mail: karlina@mail.ioffe.ru*

Received July 5, 2022; revised November 17, 2022; accepted November 22, 2022

Abstract—The possibility of controlling the composition of lateral nanowires by the method of growth under quasi-equilibrium conditions in a quasi-closed volume from indium, phosphorus, and arsenic vapors with Au catalyst in the “vapor-liquid-solid” mechanism has been demonstrated for the first time. It has been experimentally shown that the additional presence of arsenic in the indium-phosphorus source leads to the coalescence of catalytic gold droplets at the initial stage of the growth, which determines the further morphology and growth kinetics of nanostructures. An additional formation of indium phosphide nanostructures with a composition different from that of the main nanowires was found. The results of the studies expand the possibilities of the developed method for obtaining lateral nanowires on gallium arsenide substrates.

Keywords: InGaAsP lateral nanowires, “vapor-liquid-solid” growth mechanism, Raman spectroscopy, photoluminescence

DOI: 10.1134/S1063782623080067

1. INTRODUCTION

Recently, along with an intensive study of vertical nanowires (NWs) of semiconductor compounds $A^{III}B^{V}$, there is a growing interest in the study of planar (lateral) nanowires, which can ensure compatibility with planar technology both based on $A^{III}B^{V}$ and silicon compounds. These lateral nanostructures can be used for various devices, including solar cells, optoelectronic converters, field-effect transistors [1–4].

A large number of papers related to the study of the growth kinetics of nanowires by various methods, but the results obtained mainly describe the regularities of the formation of vertical nanowires. It is known that the flows of V group elements (arsenic and phosphorus), and their ratios actively influence not only the structure of the growing layers, but also the rate of their growth. There is a theoretical model for the nanostructures growth that takes into account the influence of arsenic and phosphorus flows on the rate and structure of vertical NWs [5].

Successful application of NWs in practice requires a predictable composition of the structure, morphology, and rate of the grown layers. An attempt to make a model of vertical nanowires growth for the system III—$P_{1-x}As_x$ using gold as a catalyst was made in the paper [6]. The developed thermodynamic and kinetic approaches made it possible to determine clear ways for the necessary composition control of nanowires based on III—$P_{1-x}As_x$ with a possible extension to other systems of materials.

The growth of lateral NWs has significant features. First of all, these structures are epitaxially bonded to the substrate, and the composition of the catalytic droplets is also formed as a result of subdissolution of the substrate. In papers [7, 8], the kinetics and growth mechanism of lateral nanostructures are analyzed and it is shown that the growth rate of planar whisker wire nanocrystals can be limited either by the Gibbs-Thomson effect (at small catalyst droplet sizes) or by diffusion of adatoms from the substrate surface (upon crystal radius increasing). The model under consideration [7] assumes a large scattering of NW lengths (growth rates) due to the effect of the following factors:

(1) variation of the incubation time until the nucleation of NWs,

(2) variation in the growth termination time of various NWs, caused by the spatial heterogeneity of the vapor flow,

(3) stochasticity of the growth process.

In this case, the growth rate of planar NWs is determined by the competition between the Gibbs-Thomson effects in the droplet and surface diffusion, which leads to a nonmonotonic dependence of the NW length on the radius. The mechanisms of diffusion growth of planar NWs differ from those for vertical ones, which leads to a difference in the exponents of the dependence of the growth rate on the radius [7, 8].

Specially note that in the course of annealing, gold droplets can deepen into the surface of the substrate, and the "exit" from this deepening is the incubation time. The variation in the incubation time until NW nucleation is the main reason of the different growth rates. The incubation process is preceded by the formation of catalytic droplets, if we use deposited layers of gold, which at the initial stage of the growth process form these catalytic droplets. It is known that in a number of cases coalescence of these droplets occurs, leading to their even more heterogeneous size distribution [9].

Thus, the existing models do not fully take into account all the processes that occur during the growth of lateral NWs under the "vapor-liquid-solid" mechanism, and therefore it is necessary to have additional experimental data on the conditions for the formation of catalytic droplets and the composition of the grown NWs caused by a change in the composition of the vapor phase. Previously, we shown the successful application of lateral NWs as antireflection coatings for devices based on gallium arsenide from source Sn–InP [10].

Obtaining lateral nanostructures by the method proposed by us is based on catalytic growth by the vapor-liquid-crystal mechanism from sources Sn–InP or In–InP using gold droplets as a catalyst [10]. In this case, the composition of the catalytic droplet includes the elements Au–Ga–In–P–As. At that, the content of arsenic and gallium in the catalytic droplet, from which growth occurs, is determined by the balance between the supply of As and Ga into the catalyst droplet (Au) due to the substrate dissolution and the desorption of Ga and As atoms from its surface. Thus, the composition of the resulting NWs is determined by the temperature and time of the process.

This work is aimed at revealing the possibility of controlling the composition of NWs by changing the composition of the vapor phase and is experimental study of the effect of arsenic and phosphorus in the composition of the source on the kinetics of the catalytic droplets formation, the growth of lateral NWs, and their composition. The main task was to obtain NWs of various compositions using the catalytic growth method developed by us under quasi-equilibrium conditions.

2. EXPERIMENT PROCEDURE

Polished GaAs (100) "epi-ready" quality plates were used as substrates. Initial deposition of Au (catalyst) films was carried out by magnetron sputtering. The growth of lateral structures was carried out in a quartz reactor with a graphite cassette in a hydrogen atmosphere. The reactor design contains special graphite evaporator cells with a melt solution of InP in Sn. Vapors of indium and phosphorus were directed through an opening in the lower part of the cell to the samples located directly under the evaporation cells (a quasi-closed volume). The procedure is described in more detail by us in the paper [10].

A significant difference between these experiments and those presented earlier is the change in the composition of the source Sn–In–P, to which a certain amount of InAs was added in the form of a saturated solution-melt of In–InAs in various ratios (from 20 to 35 wt % *n*-As). Measurements of the source composition showed that the content of indium in the melt practically does not change, in other words, a change in the concentration of the components of the V group does not affect the solubility of indium in tin. In this way, the composition of the vapor phase and the ratio of arsenic and phosphorus in it were changed, which made it possible to additionally control the composition of growing nanostructures. In this study, the GaAs substrate was under the source from the very beginning of the process. After reaching the desired process temperature, the substrate remained under the source for a certain time, after which it was removed from the growth zone.

The chemical composition of the source before and after growth was determined by X-ray electron probe microanalysis using a microanalyzer Camebax (CAMECA, France) equipped with a wave dispersive analyzer. Quantitative analysis was carried out using microanalyzer software. The study of the source composition made it possible to determine the ratio of flow of elements V/III as ~ 8–10/1.

The surface morphology of produced samples was studied by scanning electron microscopy (SEM) method using a Carl Zeiss SUPRA25 microscope equipped with an energy dispersive spectrometer Ultim. The elemental composition of lateral nanostructures grown on the GaAs surface was determined by energy dispersive (EDX) analysis in plan view and isometry modes at an electron beam accelerating voltage of 10.5 kV.

The Raman scattering spectra of light were obtained in the backscattering geometry in polarization $z(xy)\bar{z}$ on unit with spectral resolution 1 cm^{-1} minimum. For excitation a single-frequency cw laser with a wavelength of 532 nm was used.

The photoluminescence spectra were measured using the same spectral unit through a lens with 80× magnification to ensure high spatial resolution.

3. RESULTS AND DISCUSSION

Figure 1 shows typical electron microscopic images of the surface of the grown lateral structures. Catalytic droplets on GaAs(100) substrate were formed by sputtering of Au layer 5 nm thick by magnetron sputtering followed by annealing at a temperature of 400°C for 3 min and had a diameter of 40 to 120 nm. Further, the obtained plate was divided into two parts. One part was a control sample and the growth of lateral nanostructures was carried out from a saturated Sn–In–P melt solution. The vapor phase composition for the second half of the substrate contained an additional amount of arsenic. Thus, NW samples were obtained under the same temperature-time conditions, with initially identical Au catalytic droplets, but with different source compositions (Fig. 1a—source Sn–In–P, 1b—Sn–In–P–As).

The amount of arsenic in the source was less than or equal to the amount of phosphorus and amounted to tenths of atomic percent after the NW growth process. The composition of the catalytic droplets after the growth process was also analyzed. Studies showed that the droplets include Au–Ga–In–As–P in various proportions. The gallium concentration in the droplet usually varies from 15 to 40%, while the indium concentration is noticeably lower. The arsenic concentration always exceeded the phosphorus concentration. The additional arsenic addition to the source had practically no effect on the composition of the catalytic droplet.

As can be seen from the Figure, during the catalytic growth of nanostructures using the Sn–In–P source under the chosen conditions, the sample has almost continuous film as a result of the fusion of individual nanowires. As was shown earlier, in this case the catalytic droplets are depleted due to accelerated crystallization at the droplet-crystal interface at the corresponding ratio of phosphorus and arsenic in the droplet [11]. Thus, the radial growth of planar nanowires occurs due to the atoms incorporation into the side walls of crystals and their association. A somewhat different picture is observed when arsenic is added to the Sn–In–P source. As the arsenic content in the vapor phase increases, the catalytic droplets exhibit a clear tendency to coalesce, resulting in larger droplets. Thus, the size of these catalytic droplets directly depends on the coalescence process at the initial stage of NW growth. In contrast to the experimental conditions described in [9], where, according to the authors opinion, the determining factor in the process of droplets coalescence was the thickness of the metal film during their formation, in our experiment the droplets were already formed in advance, and their coalescence occurred directly under the source at the beginning of the growth process. In this case, the initial distribution of catalytic drops was the same for both samples. The difference in the conditions of NW growth from source containing additional amount of arsenic consisted only in changing the ratio of the V group elements in the vapor phase.

It can be assumed that the migration of catalytic droplets, leading to their coalescence, is due to a change in surface tension as a result of a significant change in the composition of the vapor phase. In order to minimize the total surface energy, small droplets of a certain diameter tend to aggregate and form larger droplets precisely through coalescence.

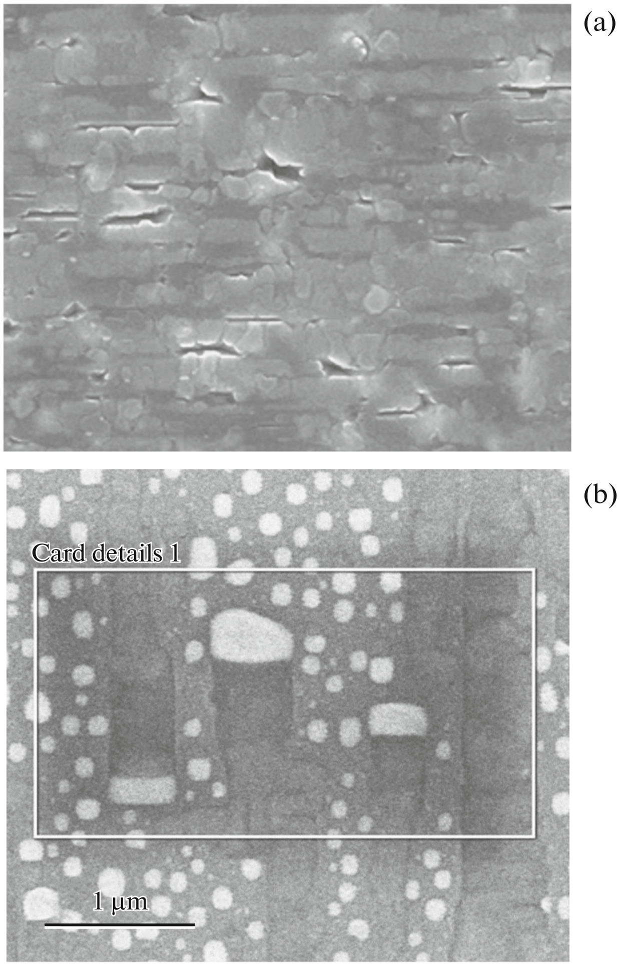

Fig. 1. Electron microscopic image of the surface of lateral nanostructures with different source compositions: (a) Sn–In–P, (b) Sn–In–P–As.

In our experiment, a noticeable growth of nanowires was observed only in the case of the motion of large-diameter catalytic droplets. Droplets of smaller diameter remained practically immobile.

The dependence of the NW growth rate on the size of catalytic droplets was repeatedly studied for various systems, including the compounds $A^{III}B^{V}$, ZnO, In_2O_3, PbSe [7, 12, 13]. A theoretical analysis of the NW growth kinetics of compounds $A^{III}B^{V}$ according to the vapor-liquid-crystal mechanism shows that the factors responsible for the growth rate are adsorption and desorption elements of the V group, the entry of atoms of the III group into the droplet, as well as the nucleation of nuclei at the liquid-crystal interface. The coalescence processes observed by us significantly reduce the growth rate, since they increase the nucle-

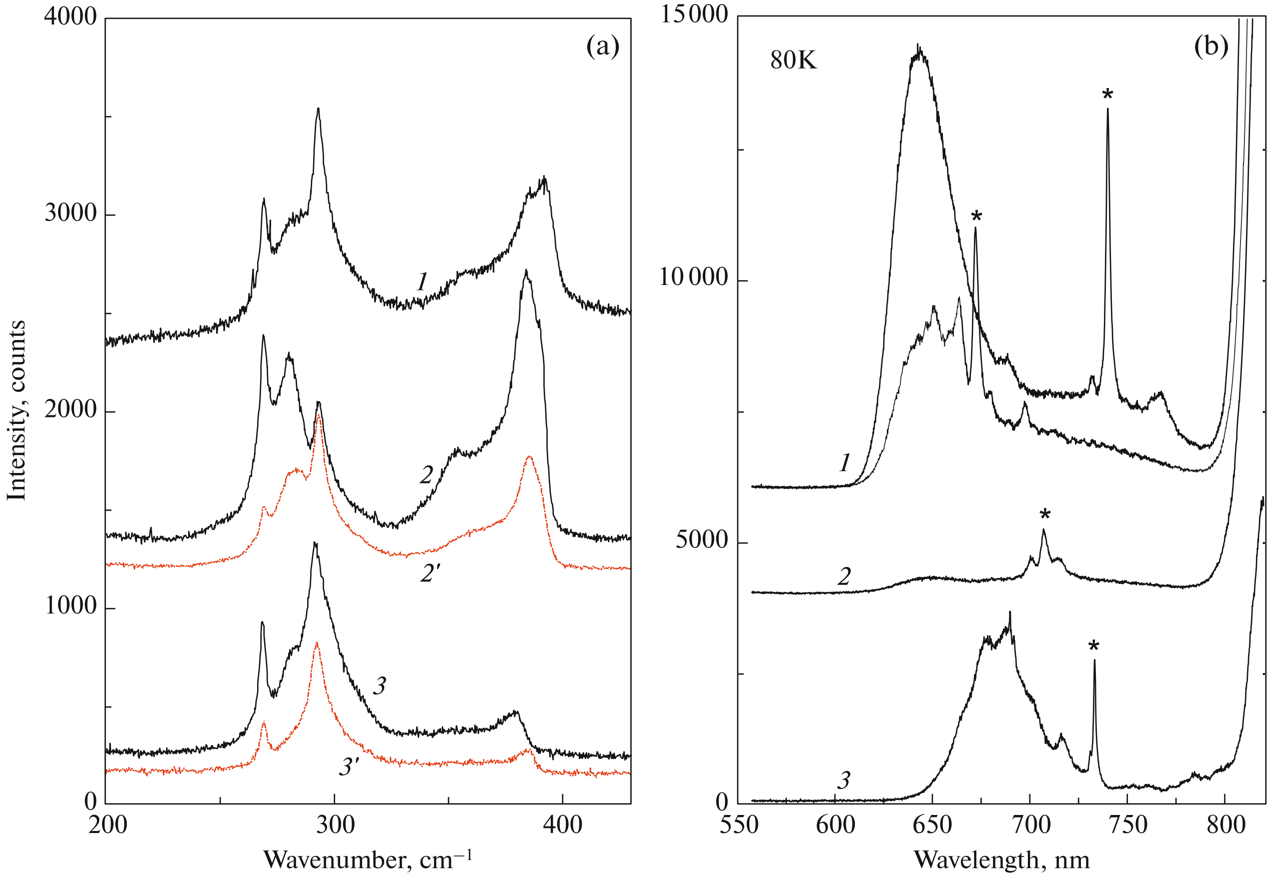

Fig. 2. Raman scattering spectra (a) and photoluminescence spectra (b) of NW samples grown from Sn–In–P melt (curve *1*), Sn–In–P–As (curve *2*) and Sn–In–P–2As (curve *3*). The dotted line in Fig. 2a shows the spectra of samples grown from the melt Sn–In–P melt, in which the growth process was stopped at an earlier stage corresponding to the state of the studied samples.

ation time at the liquid-crystal interface. In our case, the introduction of arsenic directly into the source has little effect on the composition of the catalytic droplet, but significantly increases its adsorption on the surface of lateral NWs, resulting in increase in its amount in the grown structures.

Figure 2a shows a series of Raman scattering spectra of samples grown with different amounts of arsenic. Curve *1* in Fig. 2a—spectrum of the control sample grown from vapor In, P. Two longitudinal vibrations of the GaP-type (385 and 392 cm^{-1}) can be distinguished in the spectrum, corresponding to two phases with a phosphorus content of 55 and 70%. The successive formation of two phases was described by us earlier during the Sn–In–P growth from melt [10]. In this case, first of all formation of continuous layer (consisting of individual nanostructures) of the composition XP ~ 55% is observed and its subsequent recrystallization into a layer of a larger composition with XP ~ 70%.

The presence of longitudinal vibration of the InP type (356 cm^{-1}) can also be noted in the spectra. InAs introduction into the source consistently leads to both general decrease in the NWs growth rate and increase in the arsenic content in lateral nanostructures compared to those structures that were grown using the Sn–In–P source. The lines *2* and *3* in Fig. 2a correspond to the spectra of the samples with the addition of one or two doses of InAs, respectively. It can be seen that when the first InAs dose is added, the sample is in the state of the beginning of phase 2 formation, two doses – the initial stage of phase 1 formation [10]. Corresponding spectra from samples grown without InAs addition (lower process time and/or temperature) are shown with a red dotted line. Based on the frequency dispersion of GaP-type vibrations, we can conclude that the composition of the NW solid solution changes from 55% (source Sn–In–P) to 45% (source Sn–In–P–2As).

Figure 2b shows the PL spectra of the studied samples. The spectrum contains a signal from the main phase (640–685 nm) and the GaAs substrate (820–850 nm). It can be seen that changes in the NW composition observed in the Raman spectra lead to a corresponding shift of the PL band from 640 nm (control sample) to 685 nm for the sample with the maximum content of As. The band shift of by 45 nm corresponds to composition change by 10%, which is in complete

Table 1. Composition of the sample grown from Sn–In–P–As melt at two points: GaInAsP and InP NWs (EDX)

at %	Dot 1	Dot 2
Ga	44.1	0
In	3.9	43.4
P	21.1	31.3
As	30.9	0
Au	0	25.3

agreement with the estimates made from the Raman scattering spectra.

The change in the intensity of the main band is of interest. In sample 2 (Sn–In–P–As), the PL intensity is significantly lower than in sample 1 (Sn–In–P), which corresponds to decrease in the amount of material of grown NWs. According to SEM measurements and Raman scattering spectra, in the sample 3 the NW density is even lower, but in this case, a noticeable increase in the PL intensity is observed, indicating a transition to direct-gap NW compositions, i.e. maximum ~ 50% for phosphorus. Besides, the spectra of all samples contain narrow bands, the position of which can randomly change in the range of 650–800 nm. The probability of detecting such nanoinclusions decreases with the arsenic addition to the source, i.e., with partial pressure decreasing of phosphorus. The most probable nature of these bands is the formation of InP nanoclusters, the emission of which is controlled primarily by the size effect.

The existence of InP clusters is confirmed by electron microscopic analysis data. The Table 1 presents data obtained from the EDX spectra in two different NWs on the surface of one sample. The measurement was carried out at small angles in the direction of nanostructure growth to minimize the contribution from the substrate. The point 1 corresponds to the NW formed from a large catalyst droplet (basic composition) and consists of a GaInAsP solid solution. Point 2 is an example of the growth existence without the substrate dissolution (small droplet) and contains mainly indium and phosphorus only. Note that the experimental conditions do not allow one to estimate the NW composition with sufficient accuracy; however, it clearly demonstrates the differences in the behavior of catalyst droplets of different sizes.

4. CONCLUSION

Thus, we shown the possibility of controlling the composition of lateral InGaAsP NWs by changing the composition of the vapor phase under quasi-equilibrium conditions by additional arsenic introduction into the Sn–In–P source. This opens up additional opportunities for this method use for growing NWs of various compositions. It was found that when gold films are used to form catalytic droplets, their coalescence is observed at the initial stage of growth, which depends on the state of the vapor phase, i.e., the ratio of phosphorus and arsenic.

ACKNOWLEDGMENTS

Studies using X-ray spectral microanalysis were carried out at the Center of Collective Use "Materials science and diagnostics in advanced technologies" (Ioffe PTI of RAS).

CONFLICT OF INTEREST

The authors declare that they have no conflicts of interest.

REFERENCES

1. Ch. Zhang, X. Miao, K. D. Chabak, X. Li. J. Phys. D: Appl. Phys., **50**, 393001 (2017).
2. P. C. McIntyre, A. Fontcuberta, I. Morral. Materials Today Nano, **9**, 100058 (2020).
3. Y. Wang, X. Zhou, Z. Yang, F. Wang, N. Han, Yu. Chen, J. C. Ho. Crystals, **8**, 347 (2018).
4. S. Mohammad, M. Kashani. NanoExpress, **2**, 020012 (2021).
5. V. G. Dubrovskii. J. Cryst. Growth, **440**, 62 (2016).
6. V. G. Dubrovskii. J. Cryst. Growth, **498**, 179 (2018).
7. A. Rothman, V. G. Dubrovskii, E. Joselevich. PNAS, **117** (1), 152 (2020).
8. V. G. Dubrovsky, I. V. Shtrom. Pis'ma ZhTF, **46** (20), 15 (2020) (in Russian).
9. D. Lai Guo, X. Huang, G. Zh. Xing, Zh. Zhang, G. P. Li, M. He, H. Zhang, H. Chen. Phys. Rev. B, **83**, 045403 (2011).
10. A. S. Vlasov, L. B. Karlina, B. Ya. Ber, N. A. Bert, M. E. Boiko, D. Y. Kazantsev, A. A. Levin, A. B. Smirnov, I. P. Smirnova, I. P. Soshnikov. Materials Today Commun., **31**, 103232 (2022).
11. Yu. Zhang, A. M. Sanchez, Y. Sun, J. Wu, M. Aagesen, S. Huo, D. Kim, P. Jurczak, X. Xu, H. Liu. Nano Lett., **16**, 1237 (2016).
12. V. G. Dubrovsky, A. S. Sokolovsky, H. Hijazi. Pis'ma ZhTF, **46** (17), 26 (2020) (in Russian).
13. P. D. Markowitz, M. P. Zach, P. C. Gibbons, R. M. Penner, W. E. Buhro. J. Am. Chem. Soc., **123** (Pe19), 4502 (2001).